FAST MARCHING THE GLOBAL MINIMUM OF ACTIVE CONTOURS

Laurent D. COHEN

CEREMADE, U.R.A. CNRS 749
Université Paris 9 - Dauphine
75775 Paris cedex 16, France
cohen@ceremade.dauphine.fr

Ron KIMMEL

Lawrence Berkeley Laboratory
University of California
Berkeley California 94720, USA
ron@csr.lbl.gov

ABSTRACT

A new approach of edge integration for shape modeling is presented. It is used to find the global minimum of an active contour model's energy between two points. Initialization is made easier and the curve is not trapped at a local minimum by spurious edges. We modify the "snake" energy by including the internal regularization term in the external potential term. Our method is based on the interpretation of the snake as a path of minimal length in a Riemannian metric, or as a path of minimal weighted distance. We then make use of a new numerical method to find the shortest path which is the global minimum of the energy among all paths joining the two endpoints. We show examples of our method applied to real aerial and medical images.

1. INTRODUCTION

Variations of the active contour model ('snakes') for boundary integration and features extraction, introduced in [1], have been considerably used and studied during the last years. Although the smoothing effect of the snakes may overcome small defaults in the data, spurious edges generated by noise or in a complex image may stop the evolution of the curve so that it might be trapped by an insignificant local minimum of the energy. The inflation or expansion force [2] helps to overcome such difficulties.

In this paper we present some results on a new approach for finding the global minimum for energy minimizing curves. Only endpoints are needed as an easy initialization and we are guaranteed that the global minimum is found between these points and that spurious edges cannot lead to a local minimum. The minimization problem we are trying to solve is slightly different from the deformable models, though there is much in common. Following [3], we modify the snake energy in a way that makes it 'intrinsic' or free of the parameterization. The modification we follow enables us to include the internal regularization term in the external potential term in a natural way. The energy $E(\mathcal{C})$ of the new model has the following form:

$$\int_\Omega w\|\frac{\partial \mathcal{C}}{\partial s}\|^2 + P(\mathcal{C})ds = \int_\Omega \tilde{P}(\mathcal{C})ds = wL + \int_\Omega P(\mathcal{C})ds \quad (1)$$

where P is the potential associated to the external forces. Here $\mathcal{C}$ is in the space of all curves connecting two given points (restricted by boundary conditions): $\mathcal{C}(0) = p_0$ and $\mathcal{C}(L) = p_1$, where L is the length of the curve. Contrary to the classical snake energy, here s represents the arc-length parameter, which means that $\|\frac{\partial \mathcal{C}}{\partial s}(s)\|^2 = 1$. The regularization term with w, now exactly measures the length of the curve. We showed some regularization properties of this parameter in [4].

2. PATHS OF MINIMAL ACTION

Motivated by an approach of minimal path estimation on a surface [5], we use an evolution scheme that provides at each image pixel an output of the energy along the path of minimal integrated energy joining that pixel to the given start point. The search for a global minimum is then done efficiently. While this minimum is restricted to start and end between two given points, we also presented a topology–based saddle search that helps in automatically closing contours by clicking on a single point along the boundary [4].

Having the above minimization problem in mind, we first search for the *surface of minimal action* U starting at $p_0 = \mathcal{C}(0)$. At each point p of the image plane, the value of this surface U corresponds to the minimal energy integrated along a path starting at p_0 and ending at p.

$$U(p) = \inf_{\mathcal{C}(L)=p} \left\{ \int_{\mathcal{C}} \tilde{P} ds \right\} \quad (2)$$

2.1. Minimal Action Level Sets Evolution

In what follows, we assume that $P \geq 0$. Using the definition of U to minimize our energy (1), it is possible to formulate a partial differential evolution equation describing the set of equal energy contours $\mathcal{L}$ in 'time', where t is in fact the value of the energy. These are the

This work was supported in part by the Applied Mathematics Subprogram of the Office of Energy Research under DE-AC03-76SFOOO98, and ONR grant under NOOO14-96-1-0381.

level sets of U_0 defined by Eq. (2). In the evolution equation t represents the height of the level set of U_0:

$$\frac{\partial \mathcal{L}(v,t)}{\partial t} = \frac{1}{\tilde{P}}\vec{n}(v,t), \tag{3}$$

where $\tilde{P} = P + w$ and $\vec{n}(v,t)$ is the normal to the closed curve $\mathcal{L}(.,t) : S^1 \rightarrow I\!R^2$. The motivation for this evolution is that we need to propagate with a velocity that is proportional to the inverse of the penalty. So that at 'low cost' area the velocity is high while at a 'high cost' area the velocity is low.

The curve $\mathcal{L}(v,t)$ corresponds here to the set of points p for which the minimal energy $U_0(p)$ is t:

$$\{\mathcal{L}(v,t), v \in S^1\} \;=\; \{p \in I\!R^2 \mid U_0(p) = t\} \tag{4}$$

This evolution equation is initialized by a curve $\mathcal{L}(v,0)$ which is a small circle around the point p_0. It corresponds to a null energy. It then evolves according to Eq. (3), similar to a balloon evolution [2] with an inflation force depending on the potential.

It is possible to compute the surface U in several ways. We describe three of them based on level-sets and front propagation that are consistent with the continuous case while implemented on a rectangular grid.

Front Propagation Approach. Using the Eulerian formulation [6], the evolution of $\mathcal{L}(t)$ in Eq. (3) is reformulated into the evolution of an implicit representation of the curve defined by an evolving surface $\phi : I\!R^2 \times [0,T) \rightarrow I\!R$, where for each value of t, $\mathcal{L} = \phi^{-1}(0)$. This means that the curve $\mathcal{L}(t)$ is the zero level set of $\phi(t) : I\!R^2 \rightarrow I\!R$. The evolution rule of ϕ is then given by:

$$\frac{\partial \phi}{\partial t} = -\frac{1}{\tilde{P}}\|\nabla\phi\|. \tag{5}$$

Shape from Shading Approach. The second approach is based on [7] and searches for the surface U itself instead of tracking its level sets. Given $\mathcal{U} = 0$ at the start point as boundary condition, $\mathcal{U}$ follows the evolution equation:

$$\frac{\partial \mathcal{U}}{\partial \tau} = \tilde{P} - \|\nabla\mathcal{U}\|. \tag{6}$$

Then the solution U is the steady state of $\mathcal{U}(p,\tau)$ when τ is large. The limit value $U = \mathcal{U}_\infty$ is such that

$$\|\nabla U\| = \tilde{P}, \tag{7}$$

with obviously $U = 0$ at the start point.

2.2. The Fast Marching Method

In his recent report [8], Sethian presents a fast and efficient method for solving Eq. (7). It is based on a clever way for propagating the information on the grid. Motivated by the two methods above, his method uses the proposed numerical scheme in [6, 7]. However, by marching in an ordered way, the problem is solved after a finite number of steps. It is based on the fact that information is propagating from the source point 'outwards'. Following [8], the method goes as follows:

Initialization:

- For each point in the grid, let $U_{i,j} = \infty$ (large positive value). Label all points as *far*.
- Set the start point $(i,j) = p$ to be zero: $U_p = 0$, and label it as *trial*.

Marching Forward Loop:

- (i_{min}, j_{min}) *trial* point with the smallest U value.
- Label the point (i_{min}, j_{min}) as *alive*, and remove it from the *trial* list.
- For each of the 4 neighboring grid points (k,l) of (i_{min}, j_{min}):
  - If (k,l) is labeled *far*, then label it *trial*.
  - If (k,l) is not *alive*, then compute $U_{k,l}$ according to Eq. (8), selecting the largest solution to the quadratic equation, which is the only valid solution. *i.e.* solve

$$\begin{aligned}(\max\{u - \min\{U_{k-1,l}, U_{k+1,l}\}, 0\})^2 + \\ (\max\{u - \min\{U_{k,l-1}, U_{k,l+1}\}, 0\})^2 = P_{k,l}^2,\end{aligned} \tag{8}$$

and let $U_{k,l} = u$.

We refer to [8, 9, 10, 11, 4] for further details on the above algorithm, as well as a proof of correct construction. Using a min-heap structure for the *trial* list, the algorithm computational complexity is $O(N log N)$ where N is the number of grid points.

A synthetic example is presented in Fig. 1. Observe the way the level curves propagate faster along the path. In Fig. 2, we are interested in a road detection between two points. Road areas are lighter and correspond to higher gray levels. The potential function P was thus selected to be the opposite of the gray level image itself: $P = -I$. Our approach can be used

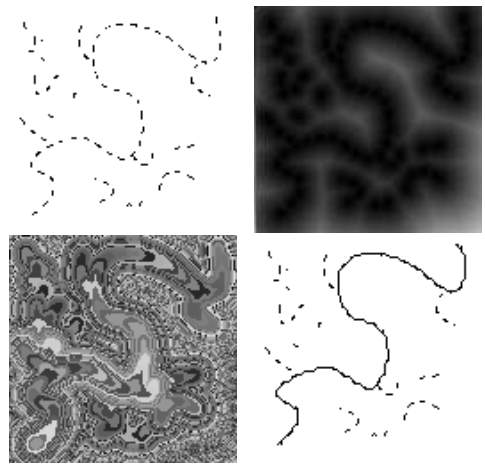

Figure 1: Line image. Top: original and potential. Bottom: level sets of U and minimal path.

Figure 2: Path of minimal action connecting the two black points. On the right, many paths are obtained simultaneously.

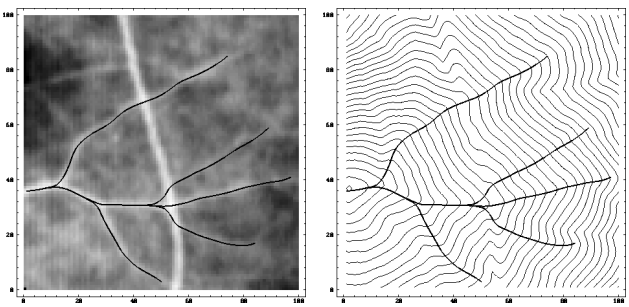

Figure 3: Finding vessels in medical angiographic image of the eye fundus. Right shows the level sets of U.

for the minimization of many paths emerging from the same point in one single calculation of the minimal action. Given a start point in the upper left area, the path achieving the global minimum of the energy is found between this point and four other given points to determine the roads graph in our previous image. Fig. 3 shows a similar result on a medical image.

3. PARAMETERIZATION AND CONVERGENCE

In several classical snakes applications the minimization is similar to Eq. (1) yet the parameter is not the arclength, i.e.

$$E_q = \int_0^1 \|\frac{\partial \mathcal{C}}{\partial q}\|^2 + P(\mathcal{C})dq, \tag{9}$$

for which the Euler equation is given by

$$\frac{\partial^2 \mathcal{C}}{\partial q^2} = \nabla P/2. \tag{10}$$

Many applications make use of this simple linear equation. However, in order to avoid node concentration and get better results, the q parameter was changed (reparametrized) into the arclength one every several iterations of the numerical scheme in [2]. Although it would appear that this was a way to obtain geometrically meaningful results, we claim that in the limit, this reparametrization leads to convergence to the intrinsic minimization only for special cases in which P is constant along the final path.

Proof. Using reparametrization via arclength s: $\frac{\partial^2 \mathcal{C}}{\partial q^2} = \frac{\partial^2 \mathcal{C}}{\partial s^2}(\frac{\partial s}{\partial q})^2 + \frac{\partial \mathcal{C}}{\partial s}\frac{\partial^2 s}{\partial q^2}$, we have in the limit $q = s$ in (10). Now, from [3], the minimization of E_q is equivalent to the intrinsic one with $\int \sqrt{E_0 - P(\mathcal{C}(s))}ds$, for which the Euler equation is

$$\frac{\partial^2 \mathcal{C}}{\partial s^2} = -\frac{\nabla P}{2(E_0 - P)}. \tag{11}$$

E_0 is an arbitrary constant that depends on the parameterization. In order for both (11) and (10) to hold we need the three following conditions to be satisfied:

- $\langle \nabla P, \frac{\partial \mathcal{C}}{\partial s} \rangle = 0$ since $\langle \frac{\partial^2 \mathcal{C}}{\partial s^2}, \frac{\partial \mathcal{C}}{\partial s} \rangle = 0$.
- $\frac{\partial^2 s}{\partial q^2} = 0$, i.e. $s = q \times$constant.
- $-\nabla P/2(E_0 - P) = \nabla P$, i.e. $P = 1 + E_0$.

The last condition indicates that P should be constant along the solution. ■

The above claim further supports our interest in geometric models.

4. GRAPH SEARCH ALGORITHMS AND METRICATION ERROR

The numerical schemes we propose are consistent with the continuous propagation rule. The consistency condition guarantees that the solution converges to the true one as the grid is refined. This is known **not** to be the case in general graph search algorithms that suffer from *digitization bias* due to the *metrication error* when implemented on a grid [12]. This gives a clear advantage to our method over minimal path estimation using graph search.

Let us review some of the graph search based methods that try to minimize the energy given in (1). A more complete survey and discussion can be found in [4]. To evaluate and minimize the snake energy [1], the "internal" terms can be evaluated only by using the shape of the curve, leading to evolution schemes from an initial curve. Based on the new energy definition (1), we are able to compute the final path without evolving an initial contour, by using the surface of minimal action. To find the surface of minimal action, graph search and dynamic programming techniques were often used, considering the image pixels as vertices in a graph [13, 14, 15].

A description of A^* and F^* algorithms, applied to road detection, can be found in [14]. The distance image is initialized with value ∞ everywhere except at a start point with value zero. At each iteration, the A^* algorithm expands to a neighbor pixel a previously

obtained minimal path ending at the vertex with smallest current cost value. Since at each iteration one pixel gets a final value, and a search for the minimal vertex to update is performed, the algorithm complexity is $O(NlogN)$ where N is the number of pixels in the image. Our approach solves a continuous version of the problem. Fast marching method [8], described in section 2.2, has a similar complexity, yet it is consistent!

The A^* algorithm searches among all vertices the one to expand at each iteration. This is why the F^* algorithm [14] was preferred in several applications, using a sequential update of the pixels. It is similar in spirit to the shape from shading approach used in Section 2.1, except that the latter is again consistent. Using the F^*, the global minimum is reached only after the image is scanned iteratively top to bottom, row by row, left to right followed by right to left, and then bottom to top. The number of such passes depends on the shape of the minimal path, which is unknown in advance in general. This kind of approach was used to compute distance maps in [16]. It was also used for road detection in [17], using some improvements in the potential definition. A simplified F^* algorithm is used in [15] to minimize a snake energy.

One may argue that using previously mentioned graph search algorithms like the A^*, Dijkstra, or F^* as proposed in [14] for road tracking, might be sufficient. These algorithms are indeed efficient, yet suffer from 'metrication errors'. As an illustration, Fig. 4 shows the isodistance curves using a graph-search approach and the continuous level-set approach. When the size of the grid is refined, these curves are always squares in the first case, while in our case, the curves are getting closer to a perfect circle.

Of course the result of the graph-search could be improved by taking a larger neighborhood as structuring element [16] or by modifying the weights [12, 18]. These give a different polygonal approximation of the circle, but there will always be an error in some direction whatever the grid resolution.

Our philosophy here is different. We propose to deal with the continuous problem as long as possible. In that, we follow the numerical analysis community, by first analyzing the underlying problem in the continuous domain. Then, at the last stage which involves numerical implementation we consider the image given as a grid of pixels, compute optimal paths and the surface of minimum action efficiently, while enjoying the 'consistency' property of converging to the desired continuous solution as the grid is refined.

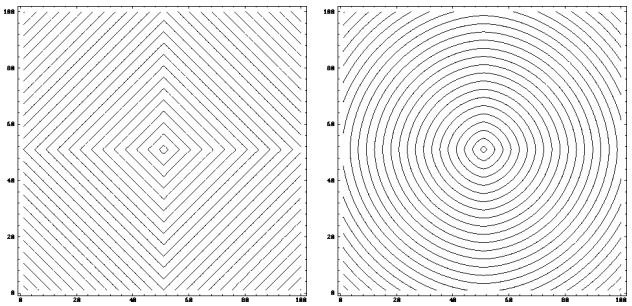

Figure 4: Metrication error: a graph search-like discrete distance on the left, our approach on the right.

References

[1] M. Kass, A. Witkin, and D. Terzopoulos. Snakes: Active contour models. *IJCV*, 1(4):321–331, 1988.

[2] Laurent D. Cohen. On active contour models and balloons. *CVGIP:IU*, 53(2):211–218, March 1991.

[3] V. Caselles, R. Kimmel, and G. Sapiro. Geodesic active contours. In *ICCV'95*, pages 694–699, Cambridge, USA, June 1995. to appear in *IJCV*.

[4] Laurent D. Cohen and Ron Kimmel. Global minimum for active contour models: A minimal path approach. Ceremade TR 9612. In part in *CVPR'96*, San Francisco, USA, and *ICAOS'96*, Paris, June 1996.

[5] R. Kimmel, A. Amir, and A. Bruckstein. Finding shortest paths on surfaces using level sets propagation. *IEEE PAMI*-17(6):635–640, June 1995.

[6] S. J. Osher and J. A. Sethian. Fronts propagation with curvature dependent speed: Algorithms based on Hamilton-Jacobi formulations. *Journal of Computational Physics*, 79:12–49, 1988.

[7] E. Rouy and A. Tourin. A viscosity solutions approach to shape-from-shading. *SIAM. J. Numer. Analy.*, 29:867–884, 1992.

[8] J. A. Sethian. A fast marching level set method for monotonically advancing fronts. *Proc. Nat. Acad. Sci.*, 93(4), 1996.

[9] J. A. Sethian. A review of the theory, algorithms, and applications of level set methods for propagating interfaces. *Acta Numerica*, 1995.

[10] D. Adalsteinsson, R. Kimmel, R. Malladi, and J. A. Sethian. Fast marching method for computing solutions to static Hamilton-Jacobi equations. Technical report, LBL UC Berkeley, 1996. submitted.

[11] R. Kimmel and J. A. Sethian. Fast marching methods for computing distance maps and shortest paths. TR, LBL, UCB, February 1996. submitted

[12] N. Kiryati and G. Székely. Estimating shortest paths and minimal distances on digitized three dimensional surfaces. *Pattern Recognition*, 26(11):1623–1637, 1993.

[13] U. Montanari. On the optimal detection of curves in noisy pictures. *Comm. ACM*, 14(5):335–345, May 1971.

[14] M.A. Fischler, J.M. Tenenbaum, and H.C. Wolf. Detection of roads and linear structures in low-resolution aerial imagery using a multisource knowledge integration technique. *CGIP*, 15:201–223, 1981.

[15] S. Chandran, T. Meajima, and S. Miyazaki. Global minima via dynamic programming: Energy minimizing active contours. In *SPIE Vol. 1570 Geometric Methods in Computer Vision*, San Diego, 1991.

[16] Gunilla Borgefors. Distance transformations in arbitrary dimensions. *CVGIP*, 27:321–345, 1984.

[17] Nicolas Merlet and Josiane Zerubia. New prospects in line detection for remote sensing images. In *Proc. of IEEE ICASSP*, Adelaide, April 1994.

[18] R. Kimmel and N. Kiryati. Finding shortest paths on surfaces by fast global approximation and precise local refinement. In *Proceedings of SPIE Vision Geometry III*, volume 2356, pages 198–209, Boston, Nov 1994.